Calcium Ions Affect the Exchange Network but not the Structure of a Small Peptide (Melanostatin) in Solution: A ^{1}H and ^{13}C NMR Spectroscopic Study

Elena Gaggelli,*[a] Nicola D'Amelio,[a] Nicola Gaggelli,[a] and Gianni Valensin[a]

Keywords: Calcium / Melanostatin / Peptides / Exchange rates / NMR spectroscopy

The interaction of calcium ions with the peptide hormone melanostatin (Pro–Leu–Gly–NH_2) was investigated by ^{1}H and ^{13}C NMR spectroscopy in [D_6]DMSO containing H_2O (1%). Chemical shifts, spin-lattice relaxation rates, ^{1}H NOESY maps and the temperature coefficients of the amide ^{1}H NMR chemical shifts were measured at increasing concentrations of calcium. A 1:1 complex with the metal coordinated to the carbonyl moieties of Pro and Gly (K_d = 17 ± 2 mM^{-1}) was shown to be the major species in solution, although evidence was also provided for the occurrence of a minor species with the metal bound to the Leu carbonyl and with different stoichiometry. Upon metal complexation, substantial changes in the intrinsic chain flexibility of the peptide and in the exchange rates between water and amide protons were detected.

Introduction

Calcium ions are widely recognized as being central to a complex intra-cellular messenger system that mediates a wide range of biological processes. Binding selectivity, allowance for irregular bond lengths and angles and the diffusion-limited reaction on-rates make calcium a suitable binder for most biomolecules, especially peptides and proteins. The relatively high concentration of calcium in extracellular fluids (close to 1 mM) has prompted investigations of its possible role in mediating interactions of flexible peptides with their macromolecular targets.[1,2] Indeed, calcium was shown to favor the interaction of carnosine with human serum albumin,[1,2] and enhance the stability of the "active" conformation in oxytocin,[3] vasopressin,[3] and bradykinin.[4] Here we show that calcium modifies the rate of exchange of an amide proton in an intrinsically flexible small peptide (melanostatin) through the intervention of the metal hydration-sphere rather than as a consequence of exposure to water of a solvent-shielded proton.

Melanostatin (MIF, melanocyte-stimulating hormone release inhibiting factor), an important tri-peptide hormone (Pro-Leu-Gly−NH_2), was chosen because of the slow exchange rate measured for the Leu-amide proton[5−8] and its biological relevance. MIF, first discovered in rat hypothalamus,[9] is generated by the enzymatic cleavage of oxytocin, and is believed to modulate dopamine-receptors in the central nervous system[10] and to inhibit the release of the melanocyte-stimulating hormone.[11,12]

All NMR spectroscopic experiments were carried out in carefully deoxygenated [$^{2}H_6$]-dimethyl sulfoxide ([D_6]DMSO) containing 555 mM H_2O (1%). This mixture was considered because it mimics critical biochemical functions, which take place away from bulk water, where molecules with hydrophilic moieties retain solvating water.

[a] Department of Chemistry, University of Siena,
Via A.Moro, Siena 53100, Italy
Fax: (internat.) + 39-0577/234-254
E-mail: gaggelli@unisi.it

Results and Discussion

Before the addition of calcium, the NMR spectroscopic features of melanostatin were typical of small flexible peptides showing no intramolecular structuring and motional averaging among different conformations. However, as previously observed,[5−8] the Leu-amide proton was found to exchange slowly with cosolvent water. Beyond the relatively large temperature coefficient of the amide ^{1}H NMR chemical shift (Table 1), a negative cross peak in NOESY and ROESY spectra was detected. While a NOESY negative cross peak may also arise from a true dipolar interaction, the negative sign in the ROESY spectrum demonstrates the occurrence of exchange only. The ratio of the cross peak to the Leu−NH diagonal peak intensity decreases almost linearly with increasing values of the mixing time, t_m (Figure 1). The surprisingly high temperature coefficient had been previously interpreted in terms of a solvent-shielded ("caged") but not hydrogen-bonded amide proton.[5−8] The remaining amide hydrogens display temperature coefficients typical of solvent-exposed protons. However, the negative cross peaks in the NOESY and ROESY spectra show slow exchange between the *syn* and *anti* protons of Gly−NH_2.

Table 1. ^{1}H NMR chemical shifts and temperature coefficients of amide protons measured for melanostatin 2.5 mM in [D_6]DMSO/water in the absence and in the presence of [Ca^{2+}] = 25 mM

Peak	δ (ppm)	Δδ/ΔT (ppm/K)[a] [Ca^{2+}] = 0 mM	[Ca^{2+}] = 25 mM
Gly−NH	8.21	−0.0050	−0.0048
Leu−NH	8.09	−0.0022	−0.0019
Gly−NH_2 (*anti*)	7.23	−0.0044	−0.0026
Gly−NH_2 (*syn*)	7.03	−0.0040	−0.0034

[a] Errors in the calculated coefficients were evaluated at ±2−3%.

  1434−1948/00/0808−1699 $ 17.50+.50/0

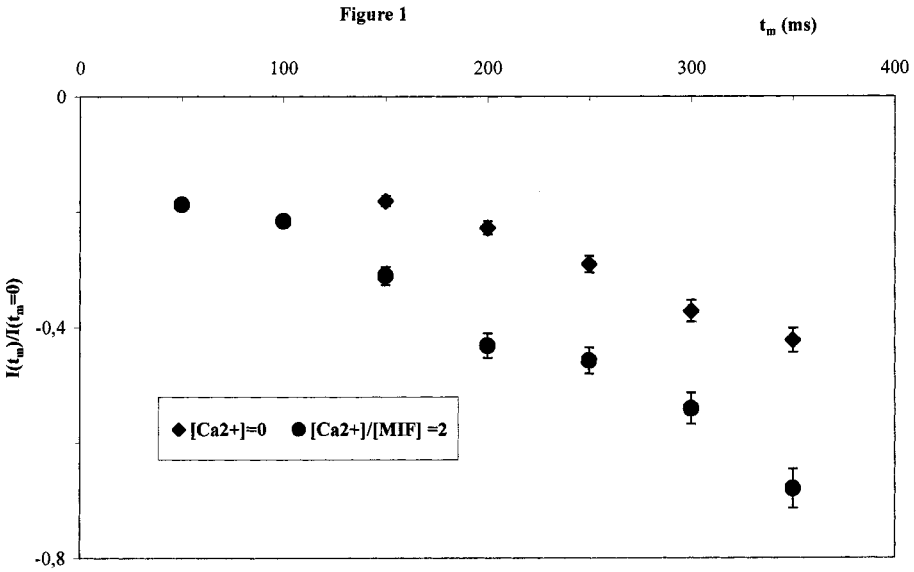

Figure 1. Intensities of the Leu−NH-water normalized exchange cross peak vs. the mixing time measured in NOESY experiments on melanostatin 2.5 mM in [D_6]DMSO/water (1%) in the absence and in the presence of Ca^{2+} 25 mM; T = 298 ± 0.1 K

Upon addition of calcium up to a ratio of [Ca^{2+}]/[MIF] = 20, several spectroscopic features were observed demonstrating formation of a 1:1 complex that substantially modifies the exchange network of the peptide with bulk water.

^{1}H and ^{13}C NMR Chemical Shifts

Both carbonyls (Figure 2 and Figure 3) and amide protons (Figure 4) were selectively affected allowing identification of the metal coordinating groups and evaluation of the dissociation constant of the complex. The Pro- and Gly-carbonyls were the most affected by the metal ion and were therefore assigned as the binding groups. It is interesting to note that two ^{13}C resonances were resolved for the Leu-carbonyl in the bound state, where the less intense of the two shifted downfield substantially. These findings seem to suggest the occurrence of a minor species, in slow chemical exchange with the major one, where the Leu-carbonyl is bound to calcium together with the Gly- or, alternatively, the Pro- carbonyls.

The titration of chemical shifts was preferably accomplished by using ^{1}H NMR spectroscopic data on amide protons that allowed several points to be obtained in a reasonable time. The exponential curves, shown in Figure 4, could be fitted to the following 1:1 binding equation [Equation (1)]with the standard regression procedure already described[13,14]

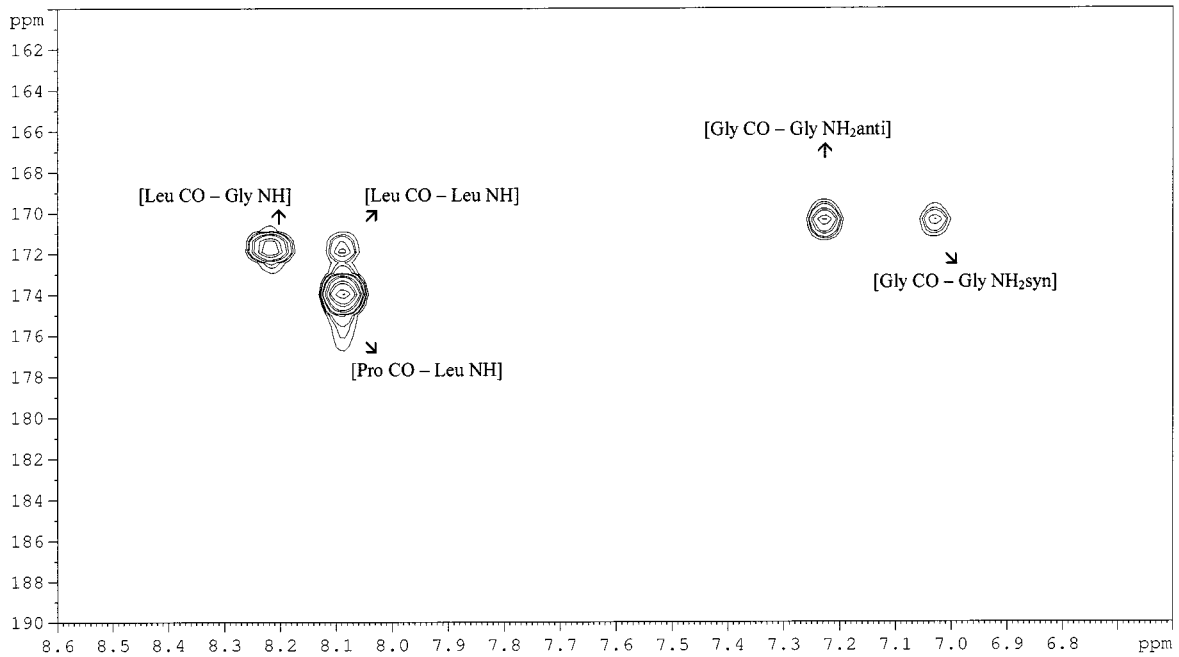

Figure 2. Low-field region of the HMBC spectrum of melanostatin 2.5 mM in [D_6]DMSO/water (1%); T = 298 ± 0.1 K

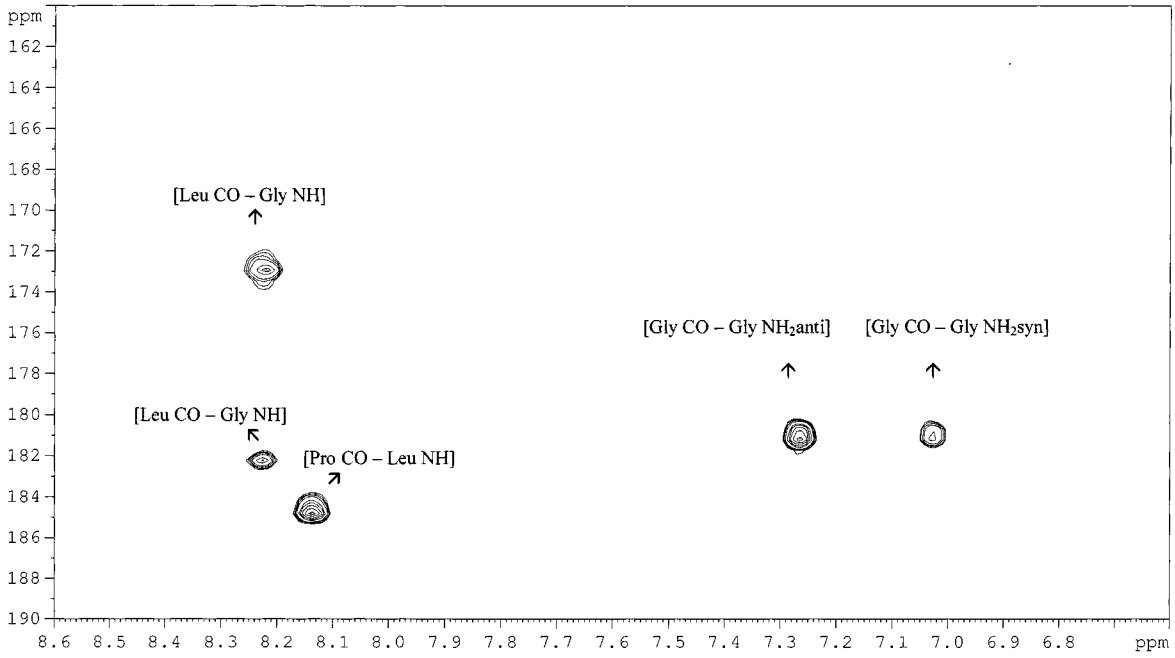

Figure 3. Low-field region of the HMBC spectrum of melanostatin 2.5 mM − Ca^{2+} 25 mM in [D_6]DMSO/water (1%); T = 298 ± 0.1 K

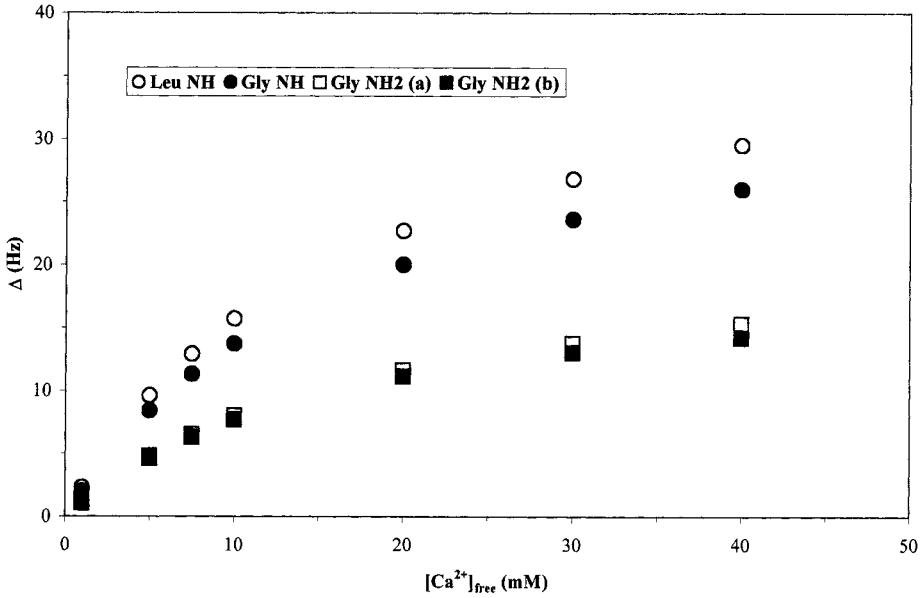

Figure 4. ^{1}H NMR downfield chemical shift changes of amide protons of melanostatin 2.5 mM in [D_6]DMSO/water (1%) vs. calcium concentration; T = 298 ± 0.1 K

$$\Delta = \Delta_0 \frac{[Ca^{2+}]_{free}}{K_d + [Ca^{2+}]_{free}} \quad (1)$$

$$\frac{\bar{\upsilon}}{[MIF]_{total}} = \frac{n}{K_d} - \frac{\bar{\upsilon}}{K_d} \quad (2)$$

where Δ is the actual change in chemical shift, Δ_0 the same change in chemical shift at the *plateau*, and K_d is the dissociation constant from the metal complex. By considering all data, K_d values in the range 0.15−0.20 mM were obtained at constant ionic strength (I = 150 mM). A Scatchard plot (not shown) was also obtained by using the experimental chemical shifts for Leu-NH and the relation shown in Equation (2)[13] where $\tilde{\nu}$ is the molar concentration ratio [MIF]/[Ca^{2+}] × Δ/Δ_0, $\tilde{\nu}/[MIF]_{total} = \Delta/(\Delta_0 - \Delta)[Ca^{2+}]_{total}$ and n is the stoichiometry of the complex. The slope and intercept from the graph of $\tilde{\nu}/[MIF]_{total}$ vs. $\tilde{\nu}$ are −5550.1 ± 11.1 and 5820.4 ± 10.6, respectively. As a consequence, the estimated values of K_d and n are ≈0.18 mM and 1, respectively. The fact that the 1:1 complex shows up as the predominant species in solution does not exclude the occurrence of different complexes in fast exchange on the NMR timescale.

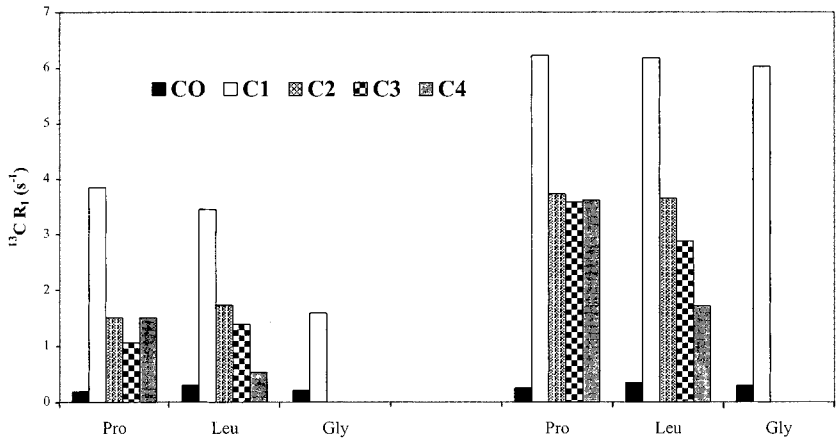

Figure 5. ^{13}C NMR spin-lattice relaxation rates of melanostatin 2.5 mM in [D$_6$]DMSO/water (1%) (left) and melanostatin 2.5 mM – Ca^{2+} 25 mM in [D$_6$]DMSO/water (1%) (right). T = 298 ± 0.1 K. Rates of protonated carbons were normalized with the number of attached protons.

^{1}H and ^{13}C NMR Spin-Lattice Relaxation Rates

Measuring ^{13}C spin-lattice relaxation rates at [Ca^{2+}]/[MIF] = 2 (Figure 5) provided the following information. In the free state, the backbone α carbons (C1 in Figure 5) display different normalized rates (R_1/n_H, where n_H is the number of protons attached to the considered carbon) and the Pro and Leu residues are characterized by the expected internal flexibility. In the calcium complex all relaxation rates are faster and, moreover, the backbone carbons are relaxed with similar rate constants and flexibility somehow reduced. The largest enhancement of relaxation rate is therefore measured for the Gly-methylene that, in the free state, was modulated by effective correlation times shorter than the other backbone carbons.

In the same manner all proton spin-lattice relaxation rates were progressively enhanced by increasing the concentration of calcium (the effect on amide protons is shown in Figure 6). In ^{13}C NMR spectroscopy the spin-lattice relaxation rates are usually determined by the dipole-dipole interaction with attached protons at a fixed distance (r_{CH} = 0.109 nm). This differs from the case of the ^{1}H nuclear spin where relaxation mainly occurs by dipole–dipole interactions with all other surrounding protons either at fixed or time-dependent distances [Equation (3)][15,16]

$$R_{1i} = \sum_{j\neq i}\rho_{ij} + \sum_{j\neq i}\sigma_{ij} + \rho_i^* \qquad (3)$$

where ρ_i* accounts for eventual mechanisms other than the dipole–dipole and ρ_{ij} and σ_{ij} are given by Equation (4)[16,17] where the interaction between any two protons i and j is averaged among all the accessible N configurations, the kth one of them being characterized by the internuclear distance r_k and the existential probability P_k. All other terms have the usual meaning: γ_H is the proton magnetogyric ratio, ω_H is the proton Larmor frequency, h is the reduced Planck constant and τ_c is the motional correlation

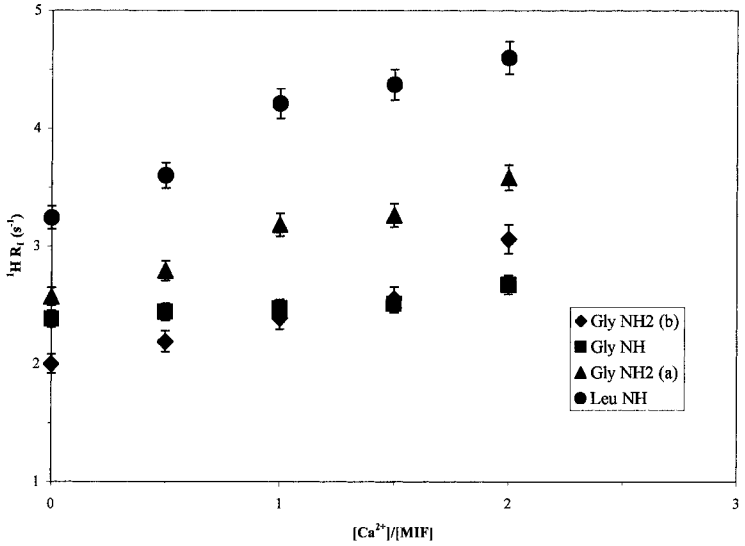

Figure 6. ^{1}H NMR spin-lattice relaxation rates of amide protons of melanostatin 2.5 mM in [D$_6$]DMSO/water (1%) vs. calcium concentration; T = 298 ± 0.1 K

$$\rho_{ij} = \frac{1}{10}\gamma_H^4\hbar^2\left\{\frac{3\tau_c}{1+\omega_H^2\tau_c^2} + \frac{6\tau_c}{1+4\omega_H^2\tau_c^2} + \tau_c\right\}\sum_{k=1}^{N}\frac{P_k}{r_k^6}$$

$$\sigma_{ij} = \frac{1}{10}\gamma_H^4\hbar^2\left\{\frac{6\tau_c}{1+4\omega_H^2\tau_c^2} - \tau_c\right\}\sum_{k=1}^{N}\frac{P_k}{r_k^6} \quad (4)$$

time. As a consequence, while the calcium-induced enhancement of ^{13}C relaxation rates can be suitably interpreted in terms of lengthened effective correlation times (vide infra), the same may not hold for protons, where changes in the number of interacting protons, internuclear distances or in ρ_i* may also be effective.

Selective (R_1^{sel}) and double selective ($R_1^{i,k}$) proton spin-lattice relaxation rates were therefore measured in order to better delineate the observed calcium induced effects. It is in fact well known that[15,18]

$$R_{1i}^{sel} = \sum_{j\neq i}\rho_{ij} + \rho_i^*$$

$$R_{1i}^{i,k} = \sum_{j\neq i}\rho_{ij} + \rho_i^* + \sigma_{ik} \quad (5)$$

Table 2. ^1H NMR relaxation rates of amide protons measured for melanostatin 2.5 mM in [D_6]DMSO/water in the absence and in the presence of [Ca^{2+}] = 25 mM

Peak	[Ca^{2+}] = 0 mM R_1/R_1^{sel}	$\sigma_{ij}\{H_j\}$ (s^{-1})	[Ca^{2+}] = 25 mM R_1/R_1^{sel}	$\sigma_{ij}\{H_j\}$ (s^{-1})
Gly−NH	1.36	----	1.09	----
Leu−NH	1.10	0.14 {Leu H_α}	1.01	−0.22 {Leu Hα}
Gly−NH_2 (*anti*)	0.59	−1.62 {Gly−NH_2}	0.62	−1.42 {Gly−NH_2}
Gly−NH_2 (*syn*)	0.64	−1.58 {Gly−NH_2}	0.66	−1.36 {Gly−NH_2}

Once measured, the new parameters (shown in Table 2) were used to delineate the effects of calcium on motional correlation times and ρ_i* through the evaluation of the ratio of nonselective to selective relaxation rates as well as on any dipole−dipole relaxation term of a proton pair σ_{ik} [Equation (6)]

$$\frac{R_{1i}}{R_{1i}^{sel}} = \frac{\sum_{j\neq i}\rho_{ij} + \sum_{j\neq i}\sigma_{ij} + \rho_i^*}{\sum_{j\neq i}\rho_{ij} + \rho_i^*} \quad (6)$$

$$\sigma_{ik} = R_{1i}^{i,k} - R_{1i}^{sel} = \sigma_{ki} = R_{1k}^{i,k} - R_{1k}^{sel}$$

The decrease of R_1/R_1^{sel} confirms that binding to calcium implies slowing down of molecular motions although different ρ_i* contributions to the relaxation pathway in the free and metal-bound states may also occur. As in the case of spin-lattice relaxation of carbons, the most affected is Gly-H_α which is thus verified to experience the largest reduction in mobility. The two obtained dipolar relaxation terms, $\sigma_{NH_2(a)-NH_2(b)}$ (-1.42 s^{-1} in the free and -1.34 s^{-1} in the metal-bound state) and $\sigma_{LeuNH-LeuH_\alpha}$, ($+0.14$ s^{-1} in the free and $+0.05$ s^{-1} in the metal-bound state), suggest that intramolecular chemical exchange provides the main relaxation mechanism for the Gly-NH_2 protons (negative σ's are obtained at each correlation time) and again that the motional correlation time in the bound state may be longer than in the free state; the dipolar relaxation rate, σ, in fact decreases and eventually becomes negative at increasing τ_c. However, any change in conformation yielding longer distances may reduce the observed rate. It is concluded that proton relaxation rates strongly suggest that binding to calcium reduces the motional flexibility of melanostatin, although other effects, namely a change in the relaxation mechanism and/or in internuclear distances, cannot be ruled out.

Temperature Dependence of Amide ^1H Chemical Shifts

The surprisingly high temperature coefficient of Leu-NH (Table 1) has been previously noticed and interpreted in terms of a solvent shielded but not hydrogen-bonded amide proton. The other three protons display coefficients typical of solvent exposed protons. However, upon addition of calcium, all coefficients are progressively enhanced, especially that of the low field Gly-NH_2 proton (from -4.4 ppb/K to -2.6 ppb/K).

^1H 2D NOESY Experiments

NOESY experiments were run for the free and calcium-bound peptide at several mixing times, t_m, in the range 50−600 ms. Beyond the positive ones, the following proton pairs displayed negative exchange cross peaks in the free state with increasing volumes at increasing t_m:

(i) the *syn* and *anti* protons within the Gly-NH_2 moiety;

(ii) Leu-NH and the residual water signal (Figure 1).

This last cross peak was analyzed by considering the following exchange matrix governing the mixing process [Equation (7)][19]

$$\hat{L} = \begin{pmatrix} \left(-R_{NH}^{sel} - \rho_{NH}^* - x_{H_2O}k\right) & -x_{MIF}\left(\sigma_{NH-H_2O} - k\right) \\ -x_{H_2O}\left(\sigma_{NH-H_2O} - k\right) & \left(-R_{H_2O}^{sel} - \rho_{H_2O}^* - x_{MIF}k\right) \end{pmatrix} \quad (7)$$

where the x are mol fractions and k is the exchange rate. By considering that $R_{NH}^{sel} >> R_{H_2O}^{sel}$, ρ_{NH}* << R_{NH}^{sel}, ρ_{H_2O}* << R_{NH}^{sel}, $x_{H_2O} >> x_{MIF}$, $\sigma_{NH-H_2O} << k$, Equations 8−10 were obtained for diagonal and cross peak coefficients as a function of the mixing time[19]

$$a_{NH}(t_m) = x_{MIF}e^{-\delta t_m}\left\{\cosh(Dt_m) - \frac{\delta}{D}\sinh(Dt_m)\right\}$$

$$a_{NH-H_2O}(t_m) = x_{MIF}\frac{k}{D}e^{-\delta t_m}\sinh(Dt_m) \quad (8)$$

with

$$\delta = \frac{1}{2}\left(R_{NH}^{sel} + k\right)$$

$$D = \frac{1}{\sqrt{2}}\left(R_{NH}^{sel} + k\right) \quad (9)$$

It follows that the ratio between the intensities of cross- and diagonal peaks is given by:

$$\frac{I_{NH-H_2O}}{I_{NH}} = \frac{k\sqrt{2}}{R_{NH}^{sel} + k} \frac{\sinh\left\{\frac{1}{\sqrt{2}}\left(R_{NH}^{sel} + k\right)t_m\right\}}{\cosh\left\{\frac{1}{\sqrt{2}}\left(R_{NH}^{sel} + k\right)t_m\right\} \quad \frac{\sqrt{2}}{2}\sinh\left\{\frac{1}{\sqrt{2}}\left(R_{NH}^{sel} + k\right)t_m\right\}} \quad (10)$$

which is an almost linear function of I_c/I_d vs. t_m at constant values of k and R_{NH}^{sel}. Interestingly, as shown in Figure 1, in the calcium-bound state the intensity of the water-Leu-NH cross peak at any value of t_m was rather enhanced, while that of the other exchange peak was reduced. Analysis of the reported equation allowed two inferences, (i) $k > R$ determines that the intensity ratio almost uniquely depends upon t_m; (ii) $k < R$ yields enhancements of the intensity ratio when increasing either k or R, or both. However, the effect of increasing k (at constant R) can be calculated to overwhelm that of increasing R (at constant k). This seems to suggest that the main, but not the only, cause of the observed phenomena is to be sought in a substantial change in the proton exchange rates between the involved environments.

Conclusion

Melanostatin is a small flexible molecule that, upon binding to calcium, undergoes several NMR spectroscopically detectable changes. The main species is a 1:1 complex with Pro- and Gly- carbonyls bound to the metal ion with $K_d \approx 0.16$ mM. Minor species bound through the Leu-carbonyl were also detected (Figure 7 and Figure 8). Metal chelation brings about a sizeable increase in effective motional correlation times, modulating reorientational motions of almost all carbon-proton and proton-proton dipole-dipole vectors as deduced by the enhanced ^{13}C and ^{1}H NMR relaxation rates. Moreover, the degrees of internal flexibility are reduced and the peptide is somehow forced to assume a single conformation. The most interesting feature of the complex is the change in the intensities of exchange cross peaks. It may be speculated that in the free state, reorientational motions transiently destroy the interaction with water. In the metal-bound state the Leu-amide proton enters the proton exchange network of the flexible coordination sphere of calcium. It is hydrogen-bonded to a coordinated water molecule that rapidly exchanges with bulk solvent. That this might be the case is ratified by the enhanced temperature coefficient of the involved amide proton. In the same way the large increase in the same coefficient of the low-field Gly-amide proton suggests that the same occurs for one of the NH_2 protons, thus reducing the rate of intramolecular exchange connected to damped rotation around the C−N bond. For better delineation of structure and dynamics, the motional correlation time of the calcium complex was calculated by considering the following:

(i) the ^{13}C NMR spin lattice relaxation rates ($\tau_c = 0.11 \pm 0.07$ ns at 298 K)

(ii) the proton dipolar relaxation rate $\sigma_{LeuNH-LeuH\alpha}$ at two different frequencies ($\tau_c = 0.14 \pm 0.08$ ns at 298 K).

$\tau_c = 0.12$ ns was then used to evaluate $r_{LeuNH-LeuH\alpha}$ at 0.261 ± 0.012 nm. Other constraints were not necessary to generate the models of the complexes (shown in Figure 7 and Figure 8) by using the AMBER force field within the HYPERCHEM software package. In this figure, four of the low conformational energy structures are superimposed onto the major complex, in order to show that the structure of the Leu side chain is ill-defined; whereas the rest of the molecule is structurally well defined, especially around the

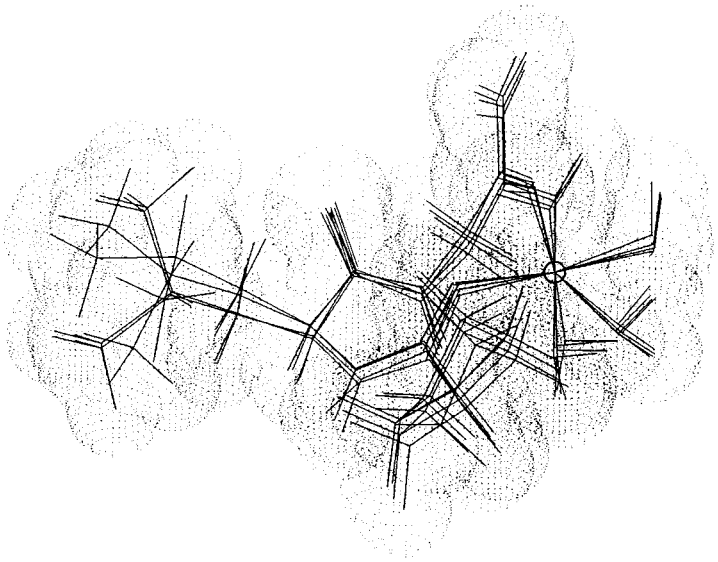

Figure 7. Superimposed stick models of four low energy structures of the main calcium-melanostatin 1:1 complex in [D_6]DMSO/water (1%); the calcium ion is circled and highlighted

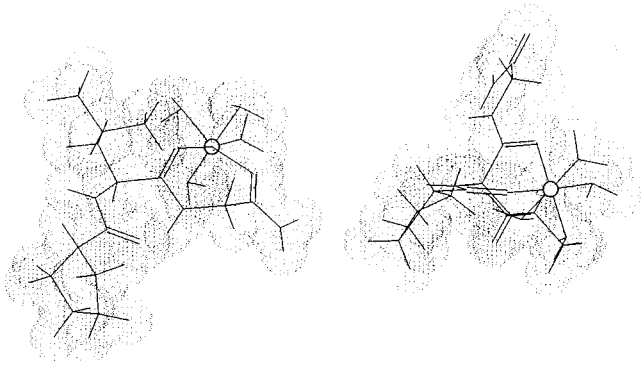

Figure 8. Stick models of low energy structures of the minor calcium-melanostatin 1:1 complexes in [D_6]DMSO/water (1%); calcium ions are circled and highlighted

metal ion (the RMSD value, calculated over the backbone atoms, was 0.06 nm).

The observed phenomena may be relevant for the biological role of calcium. Exchange of amide protons in proteins and peptides is in fact closely related to secondary and tertiary structures in solution, being the three-dimensional arrangement of any biological molecule ultimately associated with water. Backbone and side-chain hydration is a dominant factor in the stabilization of the structure, and in the process of backbone folding. It also plays an essential role in substrate binding and the mechanism of peptide and protein mediated reactions. Water diminishes charge-charge interactions and, in many proteins, has the integral role of filling cavities. Water molecules surround the molecular surface and the exchange with bulk water determines the kinetics of substrate binding or aggregation processes.

NMR 1D or 2D methods have been thoroughly exploited in discriminating solvent shielded vs. solvent exposed exchangeable protons in proteins and peptides. Exchange rates of individual amide protons in the range from reciprocal milliseconds to reciprocal months have been determined. Changes in the exchange network of backbone and side-chain protons have been consequently interpreted as demonstrating structural changes following either binding of substrates, cofactors, metal ions etc. or induced aggregation. What has been observed for melanostatin leads us to conclude that exchange rates may also be modulated by the intervention of hydration spheres of coordinated metal ions.

Experimental Section

MIF was obtained from Sigma Chemical Co. Purity of the peptide was assessed from NMR spectra and no further purification was required. Calcium perchlorate, also obtained from Sigma Chemical Co., was dried over P_2O_5 for several hours before use. Solutions were made in [D_6]DMSO containing water (1%) and were carefully deoxygenated through a freezing-sealing-thawing procedure. NMR spectroscopic experiments were carried out at 4.7 T (Varian VXR 200) and 14.1 T (Bruker Avance 600) at temperatures controlled to ± 0.1 K. Chemical shifts were referenced to internal [D_4]-trimethylsilylpropane sulfonate ([D4]TSP). NOESY experiments were carried out with standard pulse sequences at different values of the mixing time (in the range 50−600 ms). ROESY experiments were obtained at mixing times in the range 50−100 ms with the r.f. strength for the spin-lock field at values < 3.5 kHz. 2D ^{1}H-^{13}C shift correlation methods were used to detect and assign ^{13}C NMR spectra at relatively low concentration. Both ^{1}H-detected heteronuclear multiple-quantum coherence (HMQC) and ^{1}H-detected multiple-bond heteronuclear multiple-quantum coherence (HMBC) spectra were obtained with standard pulse sequences. Proton spin-lattice relaxation rates were measured with inversion recovery pulse-sequences using either non-selective, single-selective or double-selective π pulses. The rates were calculated with regression analysis of the initial decay curves of longitudinal magnetization components leading to errors in the range ±3%. Two sets of calcium titrations were performed at constant ionic strength (I = 150 mM). An approximate measure of K_d was obtained in the first set without maintaining a constant concentration of MIF.. In the second set, the peptide was added to Ca^{2+} solution to maintain a constant concentration of MIF in each NMR sample. Standard regression analysis was used to fit curves to the data by using the following equation:

$$\Delta = \Delta_0 [Ca^{2+}]_{free}/\{K_d + [Ca^{2+}]_{free}\}$$

The experimental calcium concentration was corrected thus:

$$[Ca^{2+}]_{free} = [Ca^{2+}]_{total} - [MIF]\ \Delta/\Delta_0$$

where Δ/Δ_0 is the fractional change in the chemical shift of the observed proton.[13,14]

[1] E. Gaggelli, G. Valensin, *J. Chem. Soc., Perkin Trans. 2* **1990**, 401−406.
[2] E. Gaggelli, N. Gaggelli, G. Valensin, A. Maccotta, *Bull. Magn. Reson.* **1992**, *14*, 302−306.
[3] M. Delfini, E. Gaggelli, G. Valensin, *Curr. Top. Pept. Prot. Res.* **1994**, *1*, 375−385.
[4] E. Gaggelli, N. D′Amelio, A. Maccotta, G. Valensin, *Eur. J. Biochem.* **1999**, *262*, 268−276.
[5] L. L. Reed, P. L. Johnson, *J. Am. Chem. Soc.* **1973**, *95*, 7523−7524.
[6] R. Deslauriers, R. Walter, I. C. P. Smith, *FEBS Letters* **1973**, *37*, 27−32.
[7] J. R. Garbow, C. A. McWherter, *J. Am. Chem. Soc.* **1993**, *115*, 238−244.
[8] Y. U. Sasidhar, M. M. Dhingra, A. Saran, *Indian J. Biochem. Biophys.* **1990**, *27*, 69−75.
[9] R. M. Nair, A. J. Kastin, A. V. Schally, *Biochem. Biophys. Res. Comm.* **1971**, *43*, 1376−1381.

[10] R. K. Mishra, S. Chius, P. Chiu, C. P. Mishra, *Methods Find. Exp. Clin. Pharmacol.* **1983**, *5*, 203−233.
[11] A. V. Schally, A. J. Kastin, *Endocrinology* **1966**, *79*, 768−772.
[12] M. E. Celis, S. Taleisnik, R. Walter, *Proc. Natl. Acad. Sci. USA* **1971**, *68*, 1428−1433.
[13] J. Reuben, *J. Am. Chem. Soc.* **1973**, *95*, 3534−3539.
[14] C. K. Vishwanath, K. R. K. Easwaran, *Biochemistry* **1981**, *20*, 2018−2023.
[15] R. Freeman, H. D. W. Hill, B. L. Tomlinson, L. D. Hall, *J. Chem. Phys.* **1974**, *61*, 4466−4473.
[16] J. H. Noggle, R. E. Schirmer, *The Nuclear Overhauser Effect* Academic Press, New York, **1971**.
[17] J. Tropp, *J. Chem. Phys.* **1980**, *72*, 6035−6043.
[18] L. D. Hall, H. D. W. Hill, *J. Am. Chem. Soc.* **1976**, *98*, 1269−1270.
[19] J. Jeener, B. H. Meier, P. Bachmann, R. R. Ernst, *J. Chem. Phys.* **1979**, *71*, 4546−4553.

Received November 11, 1999
[I99374]